PROJECTED CHANGES IN LATE 21ST CENTURY TROPICAL CYCLONE FREQUENCY IN CMIP5 MODELS

K. Tory *[1], S. Chand, J. McBride. H. Ye and R. Dare

Centre for Australian Weather and Climate Research

Bureau of Meteorology

1. INTRODUCTION

Changes in tropical cyclone (TC) frequency under anthropogenic climate change are examined for twenty global models from the Coupled Model Intercomparison Project Phase 5 (CMIP5), using the Okubo-Weiss-Zeta parameter (OWZP) TC detection method (Tory et al. 2013a, hereafter T13a). The method detects the immediate large-scale conditions within which TCs form. As it does not seek to directly detect the TC, we consider it to be "process-based downscaling", in that the method detects TCs by identifying the resolvable processes necessary for TC formation. The OWZP was developed and tuned in atmospheric reanalysis data, and verified against individual storms. All adjustments since the first published description, have been re-verified against individual observed TCs and then applied without further change to the climate models to ensure model and detector independence. Changes in TC frequency are determined by comparing TC detections in the CMIP5 historical runs (1970—2000) with high emission scenario (representative concentration pathway 8.5, rcp85) future runs (2070—2100). The study builds on earlier work (Tory et al. 2013b, hereafter T13b) that reported on projections from thirteen of the twenty models.

While the results are consistent with results from previous generations of climate models, they are at odds with conclusions from two recent publications by Emanuel (2013, hereafter E13) and Camargo (2013, hereafter C13). Given the level of public interest in this subject it is imperative that the differences in results be investigated further, to understand what the detectors are detecting, and the sensitivity of projection results to threshold choices. It is also important to understand what is changing in the models that leads to the differences in detections between the future and historical scenarios.

In this paper we focus on the OWZP detection technique, and begin with a summary description in Section 2. The main projection results from the 20 models are presented in Section 3. A comparison with the E13 and C13 projections is described in Section 4, along with a brief discussion of the atmospheric changes that might be responsible for changes in TC frequency. Results are summarized in Section 5.

2. PROJECTION METHODOLOGY

2.1 OWZP detections

Inspired by the marsupial pouch concept of Dunkerton et al. (2009), T13a devised a parameter to identify the core of wave-relative, nearly-closed circulations within which TCs form. The parameter is the product of absolute vorticity, and the Okubo-Weiss (OW) parameter normalised by relative vorticity (vertical components) which they termed OWZ.

$$OWZ = sgn(f) \times (\zeta + f) \times max\left[\frac{\zeta^2 - (E^2 + F^2)}{\zeta^2}, 0\right] \quad 1.$$

Here f is Coriolis, ζ is relative vorticity, $E = u_x - v_y$ the stretching deformation, $F = v_x + u_y$ the shearing deformation, and the subscripts x and y represent zonal and meridional gradients. The term is multiplied by the sign of f to ensure positive values for cyclonic flow in both hemispheres. Only positive values of the normalized OW are included, so that OWZ ranges from 1 for solid body rotation to zero when deformation exceeds vorticity. Thus, the OWZ is essentially the absolute vorticity scaled by the degree of deformation in the flow (e.g., OWZ = 0 for shear vorticity, and OWZ = $\zeta + f$ for solid body rotation.

T13a demonstrated that 95% of TCs in a 20 year selection of IBTrACS (Knapp et al., 2010) global TC data had elevated levels of OWZ on both the 850 and 500 hPa pressure levels in European Centre for Medium-Range Weather Forecasts Interim Re-Analysis (ERA-Interim) data at the time of formation. They further demonstrated that thresholds of OWZ in combination with moisture and shear thresholds (termed the OWZ

---
[1] *Corresponding author address:* Kevin J. Tory, Centre for Australian Weather and Climate Research, Bureau of Meteorology, GPO Box 1289 Melbourne, Vic 3001 Australia; e-mail: k.tory@bom.gov.au.

parameter, OWZP) could be used to detect TCs in coarse resolution numerical model data.

These thresholds describe immediately favourable conditions for TC formation. When the conditions have been favourable for at least 48 hours a tropical cyclone is deemed to have formed. The advantage of this detection method over more traditional methods is that it does not need to resolve a TC-like circulation to detect the TC, and in theory the threshold values should be independent of model and grid-resolution.

The results presented in this paper use the thresholds and system set-up described in T13b.

2.2 *Tropical/Subtropical interface*

Tropical Cyclone detection algorithms typically have difficulty distinguishing between tropical and subtropical or hybrid tropical/subtropical storms. While most subtropical storms are eliminated due to exceedance of the vertical windshear threshold, a small but not insignificant number are detected by the OWZP. Rather than specifying a fixed latitudinal boundary between tropical and subtropical storms we chose to use a dynamical definition of the tropical/subtropical interface, and include only those detected storms that formed on the equatorward side of this interface. In theory this should ensure that only storms that derive the majority of their energy from the release of lower troposphere conditional instability (rather than baroclinic instability) are deemed to be tropical cyclones. The tropical/subtropical interface is defined by the subtropical jet at 200 hPa, which is typically associated with the transition from a relatively high tropical tropopause and a lower extra-tropical tropopause.

In T13b the subtropical jet axis was used to define the tropical/subtropical interface, but in recent experiments (not yet reported) it was found that using a 200 hPa wind speed threshold of 25 ms^{-1} combined with the condition that the wind speed must increase poleward, yielded a better result. (In very strong jets, the jet axis may be hundreds of km from where the upper troposphere baroclinicity begins.)

2.3 *Projection sensitivity to thresholds*

Before presenting the projection results it is worth reporting on the sensitivity of detection numbers and projections to the threshold choices. Table 1 shows decreasing global annual TC numbers between the recent and future scenarios in two models for the default OWZ threshold settings, plus two test runs in

which the thresholds are increased progressively by $10 \times 10^{-6} s^{-1}$. Given the size of the increasing threshold increments, it is not surprising that the numbers of detections drop between 20 and 40% with each set of threshold increases. Reassuringly the projected percentage changes in TC frequency in all three cases vary by only a few percent, except for the highest threshold GFDL-CM3 case. Table 1 also shows the current climate TC detections in both models for the default OWZ settings are quite similar in number and very close to observed TC formation rates, despite the different model resolutions and the detection technique being developed and tuned independently of both models.

| Global Annual TC detections for historical and rcp85 scenarios		CMIP5 model (Lon × Lat grid points)	
		ACCESS1-3 192 × 144	GFDL-CM3 144 × 90
OWZ$_{850}$=60 OWZ$_{500}$=50 (Default)	20th C	89.68	85.16
	21st C	80.77	61.71
	% change	-9.9	-27.5
OWZ$_{850}$=70 OWZ$_{500}$=60 (Test 1)	20th C	69.55	52.48
	21st C	61.46	39.16
	% change	-11.7	-25.4
OWZ$_{850}$=80 OWZ$_{500}$=70 (Test 2)	20th C	54.06	28.77
	21st C	46.74	24.29
	% change	-13.5	-15.6

Table 1: Global annual TC detections in late 20th (blue) and late 21st (red) century climate, and percent changes for ACCESS1-3 and GFDL-CM3 CMIP5 models, for the default threshold settings (top), and two test settings in which the OWZ thresholds on both the 850 and 500 hPa levels are increased progressively by $10 \times 10^{-6} s^{-1}$ (middle and lower).

2.4 *Example detected storms*

To further test the veracity of the method a number of circulations near the formation time were manually investigated. Examples from the ACCESS1-3 model are presented in Fig. 1. The panels show 850 hPa wind vectors with a selection of 850 and 500 hPa OWZ contours (that exceed the thresholds) overlayed. The upper (lower) panel shows a TC-like circulation in the eastern (western) North Pacific basin centred at 100°W, 12°N (128°E, 20°N). The upper circulation is relatively small and is pictured about two days after formation (as determined by the OWZ detector). The lower circulation is depicted at the formation time and is comparatively large, although it contracted somewhat in the next couple of days. Both show vertically-aligned near-circular OWZ anomalies with sharp gradients. The sharp gradients occur at well-defined radii of maximum wind (T13a). Thus,

these plots demonstrate vertically aligned strong circulations that extend through the low- to mid-tropopause. Strong outflow is evident at 200 hPa (not shown) suggestive of a troposphere-deep secondary circulation.

Figure 1 shows that the OWZP TC detector is capable of detecting TC-like circulations in a range of sizes. The circulation in the upper panel is close to the minimum resolvable size for this model resolution.

850 hPa OWZ (Red):C:500 hPa OWZ (Blue)
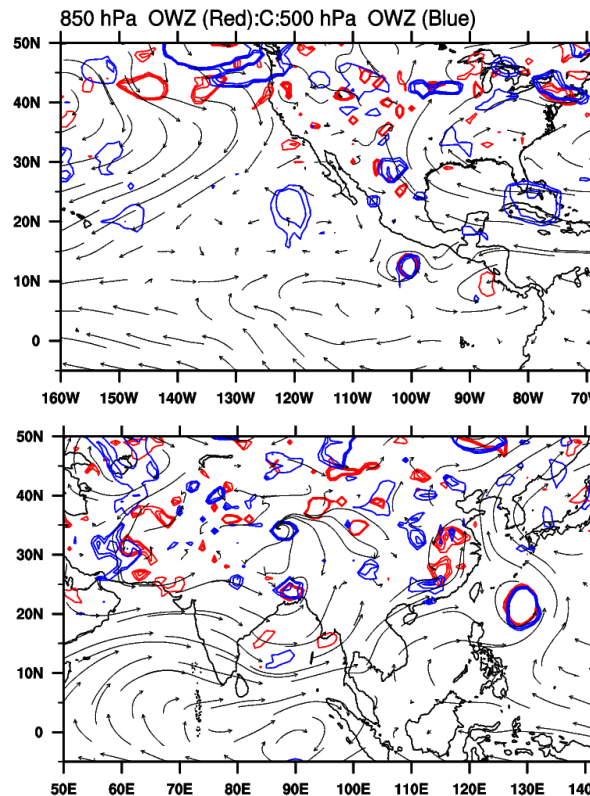
Figure 1: OWZ contours on the 850 (red, contour interval 60, 80, 100× $10^{-6}s^{-1}$) and 500 (blue, contour interval 50, 70, 90× $10^{-6}s^{-1}$) hPa pressure levels, with 850 hPa wind vectors. According to the OWZP detector, the upper panel contains a small two-day old TC at 100°W, 12°N, and the lower panel a larger TC at formation time at 128°E, 20°N.

3. PROJECTIONS

A total of twenty CMIP5 models were analysed over 31 year periods for both the historical (1970-2001) and rcp85 (2070-2100) scenarios, including the thirteen models presented in T13b. OWZP TC detections were recorded and tracked and divided into seven TC basins. However, for brevity only global results will be presented here. Table 2 lists the model name, resolution and annual global TC detection rates for each model and scenario, and the percentage change.

Model	lon×lat	20th C	21st C	% Δ
IBTrACS (Obs)		**76.2**		
MRI-CGCM3	320×160	155.2	126.8	-18.30
BCC-CSM1-1-m	320×160	68.6	73.9	7.73
CCSM4	288×192	57.1	52.3	-8.41
CNRM-CM5	256×128	48.5	44.2	-8.87
MIROC5	256×128	111.3	86.3	-22.46
ACCESS1-0	192×144	74.9	63.5	-15.22
ACCESS1-3	192×144	89.7	80.8	-9.92
HadGEM2-ES	192×144	97.5	82.7	-15.18
CSIRO-Mk3.6.0	192×96	101.2	89.7	-11.36
IPSL-CM5A-MR*	144×143	18.0	30.7	70.56
NorESM1M*	144×96	20.1	17.6	-12.44
GFDL-CM3	144×90	85.2	61.7	-27.58
GFDL-ESM2M	144×90	82.5	76.9	-6.79
GFDL-ESM2G	144×90	85.6	77.6	-9.35
CanESM2*	128×64	14.1	15.6	10.64
MIROC-ESM*	128×64	13.4	10.3	-23.13
MIROC-ESM-CHEM*	128×64	12.6	10.7	-15.08
BCC-CSM1.1	128×64	76.7	67.6	-11.86
FGOALS-g2*	128×60	21.5	31.0	44.19
IPSL-CM5A-LR*	96×96	7.5	14.1	88.00

Table 2: CMIP5 models analysed (Col 1), resolution (Col 2), global Annual TC detections, for the late 20th (Col 3) and 21st (Col 4) century and percentage change in TC detections (Col 5). High, medium and low resolution models are shaded in green, orange and red, respectively. Detections and percentage change from models with detections outside of ±50% of that observed (Row 1) are highlighted in red.

If one were to average the number of detections over each resolution category there would be a clear signal of increasing detections with increasing resolution. However, the variability is sufficiently great to illustrate that other processes (e.g., model physics) are likely to have a greater influence on detection numbers than model resolution. The most extreme example of this is the difference in detections between the high- and low-resolution BCC models, where greater detections are found in the low-resolution model, despite a 2.5 times greater grid spacing. Our visual inspection of 12 months of data from many of these models has revealed that the low-resolution models generally struggle to produce circulations that resemble TCs. The TC-like circulations they do produce are necessarily very large and can be long-lived, which presumably leads to an unrealistically large consumption of low-level conditional instability. While the detection technique may have some grid-resolution bias, we do not believe it is significant compared to other factors such as

model physics, and from the projection sensitivity tests (Section 2.3) we are confident any such bias does not affect the projections in any significant way.

3.1 *Model selection*

Like T13b we eliminate models from our projections that contain detections that differ by more than 50% from the observed global annual frequency (Table 2, Row 1). The global annual detection rate and percent change from the 20th to 21st century for these models is highlighted by red text in Table 2. Interestingly it includes all but one of the low-resolution models (red shading), and two of the medium resolution models (orange shading), all of which are due to too few detections. Only one of the high resolution models (green shading) is eliminated, and that is due to too many detections.

3.2 *Global TC frequency changes*

Ignoring the projected changes of TC frequency in red text, all but one model shows decreasing TC detections globally. The exception is the high- resolution BCC model (blue text). However, separated into hemispheres and individual basins the results (not shown) are not as consistent. No model shows a significant increase (95% confidence, see T13b for confidence testing method) TC detections in the southern hemisphere, whereas two models (BCC-CSM1-1-m and ACCESS1-3) do in the northern hemisphere. The increases in these models mostly occur in the western North-Pacific (not shown).

These results are consistent with the state of the science summary paper by a World Meteorological Organization (WMO) Expert Team (Knutson et al. 2010), released prior to the release of CMIP5 model data. However, they are at odds with two recent papers that used different detection methodologies applied to a selection of CMIP5 models (E13, C13).

4. PROJECTION CONCLUSIONS DIFFER

The general conclusion of T13b was that overall there were fewer TC detections in the high-emissions scenario (rcp85) compared with the historical scenario in the CMIP5 model runs. In contrast the general conclusions of E13 and C13 was of increased detections, and a mix of increasing and decreasing detections, respectively.

The detection method used in E13 has been described as a form of downscaling and as such is very different to the direct detection methodology of C13, which in turn is quite different to the T13a,b process-based detection method described in this paper. Thus, it is not surprising that the three methods give different results. However, it is surprising and somewhat alarming that the general conclusions differ so greatly, especially as there is great public interest in potential changes in TC behaviour.

4.1 *Detection Comparisons*

Table 3 compares the results from the three detection methodologies, where reasonable comparisons are possible. Different time periods were used in each study. The last 50, 20 and 31 years of each century were used in C13, E13 and T13b, respectively. However, there is minimal difference in the C13 results whether calculated over the last 50 or 31 years, (Camargo 2014, pers. Com.).

Model	20th C		21st C		% change		
	C	T	C	T	C	T	E
CCSM4	3	57		52		-8	+11
CSIRO-Mk3.6.0	44	101	34	90	-23	-11	
NorESM1M	2	20					
GFDL-CM3	35	85	25	62	-29	-28	+41
GFDL-ESM2M	30	83	34	77	+13	-7	
CanESM2	22	14	14	16	-36	+11	
FGOALS-g2	8	22					
IPSL-CM5A-LR	3	8					
MIROC5	14	111	8	86	-43	-22	+38
MIROC-ESM	3	13					
HadGEM2-ES	15	98	8	83	-47	-15	+22
MRI-CGCM3	58	155	70	127	+21	-18	+13
MPI-ESM-MR	28		33		+18		+29

Table 3: Twentieth and twenty-first century global annual TC detections, and percentage changes for the models reported in C13 (C), T13b and this paper (T) and E13 (E) in which comparisons can be made. Red text refers to models that reproduce current climatology poorly (as determined by the authors). Models with reasonable reproductions of current climatology that feature in the three papers are in blue text. Detections that differ by more than 2, 5 and 10 times between C and T are highlighted in grey, orange and red, respectively.

The text in blue represents the percentage change from the models in which direct comparisons can be made between all three

methodologies. For these three models the sign is negative in both C13 and T13b, but positive in E13. In fact E13 has an increase in detections for all models. Thus E13's projections agree with C13 for only the last two rows of the table: MRI-CGCM3 and MPI-ESM-MR. Interestingly, our own method (column T) produces the opposite result (reduced future detections) for MRI-CGCM3, although we have limited confidence in this result due to excessive TC detections in that model.

The other comparison that is worth making is the difference in detection numbers. (No detection numbers are available for E13, as the E13 methodology does not directly detect TCs.) First we note that T13b and C13 rejected the same models for unrealistically low numbers of detections, with two exceptions (CCSM4, CanESM2), which gives some support to our statement above that these models struggle to produce TC-like circulations. The OWZP detector systematically detects greater numbers of storms than the C13 methodology with the exception of only one model (CanESM2). In all other models the OWZP detects more than double that of the C13 detector, and more than five and ten times in the 20th and 21st centuries respectively, for two of the non-suspect models (MIROC5, HadGem2-ES).

The different philosophies behind the two detectors would suggest the OWZP method should detect more TCs than the C13 method, because the former is looking for a persistent larger-scale environment conducive to formation, whereas the latter is looking for a well-resolved anomalous cyclonic, warm-cored circulation. Valid arguments can be made for and against either method, which suggests the two methods used together can provide a spread of results that help determine uncertainty in results. However, the very significant differences in TC detection numbers demonstrate that the two detection methodologies are ascribing very different phenomena to be (or not to be) TCs. The one reassuring point is that the percent change in detections in the two methodologies are generally in agreement for the non-rejected models. It is also difficult to assess the performance of the two detectors manually (i.e., using a visual inspection of wind plots), as a subjective decision still needs to be made regarding what is and what is not a TC in the model data. A manual assessment can really only ensure that obvious non-TC-like (TC-like) circulations are not being counted, (missed) and that individual circulations are not being counted multiple times.

4.2 *Changing TC formation environment*

In addition to understanding what it is that the detectors detect, it is also important to understand what is changing in the models that leads to the changing numbers of detections, and how the individual models differ. Changes in a number of parameters that have been linked to TC formation have been investigated in a variety of CMIP5 models (e.g., C13, Tang and Camargo 2014).

In the last decade, the Emanuel and Nolan (2004) Genesis Potential Index (GPI) has been used widely in climate studies to understand seasonal changes of variables thought to be important for TC formation. C13 investigated the changing GPI, plus most of the GPI ingredients, in 14 CMIP5 models. In short, the GPI and all the ingredients investigated are in general increasing across most of the global TC formation regions (i.e., these seasonal conditions are becoming more favourable for TC formation). Six of the 14 models produced reasonable TC climatologies in our study (i.e., our "good" models), and we are able to make direct comparisons with the regional changes in OWZP detections and the GPI and its ingredients. Not surprisingly, since the OWZP projections are generally downward and the GPI changes suggest more favourable formation conditions, we found a strong signal of reduced OWZP detections in regions of more favourable seasonal GPI (not shown). We conclude from this that the seasonal GPI does not capture the important ingredients that influence the formation of circulations detected by the OWZP.

Another atmospheric quantity that has been well-correlated with TC formation is the ventilation index of Tang and Emnuel (2010). When applied to CMIP5 models (Tang and Camargo 2014) the ventilation index pointed to reduced formation favourability. Interestingly, it is a function of two of the variables in the GPI that showed increasing formation favourability, plus what they call an entropy deficit term. Hence the entropy deficit term must be large enough in magnitude to override the positive favourability of the other two terms.

Tang and Camargo (2014) investigated the changes in a ventilation index in eight CMIP5 models and found the ventilation index increased (less favourable for TC formation) across the majority of the global genesis basins. Furthermore, the numbers of days of favourable ventilation per season decreased. This is a very consistent result across all the models. Direct comparisons with our study could be made with six of the eight models. Our preliminary conclusions are that the changes in ventilation index between the future and recent climate

scenarios are very consistent with our changes in OWZP detections. Perhaps most importantly it must be the entropy deficit term (χ_m) that is responsible for the increased ventilation,

$$\chi_m = \frac{s_m^* - s_m}{s_{SST}^* - s_b},\qquad 2$$

where, s_m, s_{SST}, s_b are the moist entropies at 700 hPa, the sea surface, and the boundary layer, and * represents saturation moist entropy. E13 comment on this parameter and note that both the numerator and denominator increase under global warming but the former increases somewhat faster. This would suggest that the moist entropy deficit at 700 hPa is the only component of the ventilation index that contributes to a general, global reduction in TC formation favourability in a warming climate. This result is confirmed by Camargo et al. (2014) in a comprehensive study of genesis indices (currently under review).

Why does the 700 hPa moist entropy deficit increase in a warming climate? Climate models have shown that the relative humidity in the tropics varies little as the atmosphere warms. Thus in a warmer climate it takes more evaporation to moisten the atmosphere sufficiently for formation to become favourable (e.g., E13).

While the increased ventilation found in the CMIP5 future scenario is consistent with the reduced OWZP TC detections, it is at odds with E13. This suggests the E13 downscaling technique is not greatly influenced by changes in ventilation, and perhaps more specifically, 700 hPa moist entropy deficit.

5. SUMMARY

The OWZP process-based downscaling TC detection technique was applied to 20 CMIP5 models for the historical and rcp85 (high emission) scenarios. Projected changes in TC frequency were determined by the difference in detections between the two scenarios. Eight models were rejected from the projection analysis due to a subjectively determined unrealistic number of TC detections. All but one of the 12 remaining models show a projected decrease in detections globally.

These results are at odds with the E13 study, which showed a projected increase in all models analysed using a downscaling detection method. Using a direct detection technique C13 found mixed results, with five models showing a reduction and three models an increase in future TC detections. This lack of consistency between studies warrants further investigation. It is important that we understand what it is the various detectors are detecting, and that the projections are not overly sensitive to detector settings.

Some differences in results should be expected as the three detection techniques are very different, and they were applied over different time periods. Experiments with the OWZ threshold sensitivity demonstrated that projections based on OWZP detections are quite robust. A minor difference between the C13 study and the OWZP methodology used here is the use of a fixed latitudinal dependent tropical boundary (30°) in the former, and the dynamic tropical boundary in the latter based on the position of the subtropical jet.

The differing philosophies behind the OWZP and C13 TC detectors mean that the former should detect more TCs than the latter. However, it is of concern that the differences can be as large as 5 to 10 times, which suggests a detailed examination into what each detector is detecting is warranted.

Of all the genesis related variables investigated in CMIP5 models by C13 and Tang and Camargo (2014) (which includes the Emanuel and Nolan (2004) GPI and its ingredients) only the moist entropy deficit changes in a manner consistent with the reduced numbers of OWZP TC detections. It is important to understand what is changing in the models between the recent and future climate scenarios that leads to changes in TC detection numbers.

References

Camargo, S. J., 2013: Global and regional aspects of tropical cyclone activity in the CMIP5 models. *J. Clim.*, **26**, 9880–9902.

Camargo, S. J., M. K. Tippett, A. H. Sobel, G. A. Vecchi and M. Zhao, 2014: Testing the performance of tropical cyclone genesis indices in future climates using the HIRAM model. (under review) *J. Clim.*

Dunkerton, T.J., M.T. Montgomery, and Z. Wang, 2009: Tropical cyclogenesis in a tropical wave critical layer: Easterly waves. Atmos. Chem. & Phys., 9, 5587-5646.

Emanuel, K. A. and D. S. Nolan, 2004: Tropical cyclone activity and the global climate system. Preprints, *26th Conf. on Hurricanes and Tropical Meteorology*, Miami, Fl, Amer. Meteor. Soc., 10A.2.

Emanuel, K. A., 2013: Downscaling CMIP5 climate models shows increased tropical

cyclone activity over the 21st century. *PNAS*, **110**, 12219—12224.

Knapp, K. R., M. C. Kruk, D. H. Levinson, H. J. Diamond, and C. J. Neumann, 2010: The International Best Track Archieve for Climate Stewardship (IBTrACS) Unifying Tropical Cyclone Data. *Bull. Amer. Meteor. Soc.*, **91**, 363–376.

Knutson, T. R., J.L. McBride, J.-C. Chan, K. Emanuel, G. Holland, C. Landsea, I. Held, J.P. Kossin, A.K. Srivastava, and M. Sugi, 2010: Tropical cyclones and climate change. *Nature Geoscience*, **3**, 157-163.

Tang, B., and S. J. Camargo (2014), Environmental control of tropical cyclones in CMIP5: A ventilation perspective, *J. Adv. Model. Earth Syst.*, (Accepted Article). doi:10.1002/2013MS000294

Tory, K.J., R. A. Dare, N. E. Davidson, J. L. McBride, and S. S. Chand, 2013a: The importance of low-deformation vorticity in tropical cyclone formation. *Atmos. Chem. Phys.* **13**, 2115–2132.

Tory, K.J., S. S. Chand, J. L. McBride, H. Ye, R. A. Dare, 2013b: Projected changes in late 21st century tropical cyclone frequency in thirteen coupled climate models from the Coupled Model Intercomparison Project Phase 5. *J. Clim.*, **26**, 9946—9959.